Streaming Instability of Aggregating Slime Mold Amoebae

Herbert Levine and William Reynolds
Department of Physics and Institute for Nonlinear Science, University of California, San Diego, La Jolla, California 92093
(Received 13 November 1990)

We propose a new model of aggregation in the cellular slime mold *D. Discoideum.* Our approach couples the excitable signaling system to amoeba chemotaxis; the resultant system of equations is tractable to analytical and numerical approaches. Using our model, we derive the existence of a streaming instability for the concentric target aggregation pattern.

PACS numbers: 82.20.Mj, 05.70.Ln, 87.22.−q

Pattern formation in excitable reaction-diffusion systems is a phenomenon common to both physical and biological sciences. In the physics community, excitable systems have been the focus of research for a number of years within the context of the Belosuv-Zhabotinskii reaction[1] and more recently in the study of the catalysis of CO on Pt surfaces.[2] In biology, excitability is exhibited by many systems, including waves of cyclic adenine monophosphate (cAMP) in aggregating colonies of the slime mold *Dictyostelium Discoideum.* This system is of great interest to biologists investigating basic mechanisms of cellular interactions.[3,7] This process provides a proving ground wherein techniques developed for the analysis of physical systems can lead to insights on the mechanisms governing biological phenomena.

During the aggregation of *Dictyostelium,* the starvation of an individual amoebae sets into motion an elaborate system for the production of the signaling agent cAMP, controlled by receptors on the cell surface. The chemical signal causes the cells to move toward a common site as a precursor to slug formation, stalk growth, and sporulation (see Fig. 1). There have been several simulations of the aggregation process, using various models.[4] There has, however, been little investigation of the fundamental issue of the stability of the fully developed nonlinear signaling system.[5] Previous investigations have only considered the stability of a uniform distribution of cells and cAMP, which is *not* the relevant base state for the aggregation process. Here, we will instead consider the stability of a steady-state pulse of cAMP over a uniform cell density background to a perturbation in that density field.

Various models have been put forth to explain the detailed chemical kinetics of cAMP signaling; we will focus here on the "receptor box" model introduced by Martiel and Goldbeter.[6] Each cell has on its membrane 10^6 cAMP receptors, each of which can be in one of four states (bound or unbound, activated or deactivated). In the presence of low levels of cAMP, receptors tend to go active, while at high cAMP levels, they tend to deactivate. The activated receptors are postulated to initiate, upon binding to extracellular cAMP, an autocatalytic cAMP production mechanism within the cell. This chemical is then released from the cell and, via diffusion, can activate other cells. Meanwhile, a high level of cAMP is created, which then deactivates the receptors, which in turn causes the cAMP level to drop, thus gradually reactivating the receptors. In this manner, sustained nonlinear oscillations of cAMP are possible.

The final kinetic equations of this model are quite similar to those found in other excitable media.[8] The two variables, r and ψ, representing the fraction of activated receptors and the normalized concentration of cAMP, respectively, react on different time scales whose ratio is ϵ, a small quantity. If spatial variation of the two species is considered, then after accounting for diffusion of cAMP, one is led to a reaction-diffusion sys-

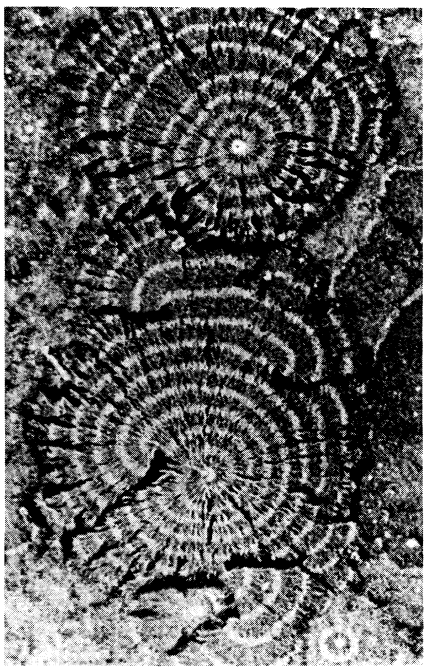

FIG. 1. Photograph of aggregating fields of *D. Discoideum.* Note the spiral signaling patterns and the onset at the aggregations' edges of the streaming instability.

tem:[9]

$$\epsilon\dot{\psi}=\epsilon^2\nabla^2\psi+f(\psi,r)\,, \tag{1}$$

$$\dot{r}=g(\psi,r)\,, \tag{2}$$

with kinetic laws $f(\psi,r)=s\Phi(\psi,r)-\psi$ and $g(\psi,r)=-f_1(\psi)r+f_2(\psi)(1-r)$, where

$$\Phi(\psi,r)=\frac{\lambda_1+\Lambda^2(\psi,r)}{\lambda_2+\Lambda^2(\psi,r)},\quad \Lambda(\psi,r)=\frac{r\psi}{1+\psi}\,,$$
$$f_1(\psi)=\frac{1+\sigma\psi}{1+\psi},\quad f_2(\psi)=\frac{L_1+\sigma L_2 h\psi}{1+h\psi}\,, \tag{3}$$

This set of equations has been used to study spiral patterns in two dimensions by Tyson *et al.*;[9] a typical set of parameters taken from this work is given in Table I. Of course, all these parameters are dependent on the cell density, which for the moment is taken to be a constant.

Following a general approach for excitable media developed elsewhere,[10,11] this system can be greatly simplified. Because ϵ is small, the system will admit a periodic wave solution in the form of excited regions followed by quiescent ones, separated by thin reaction zones ("interfaces") of width ϵ. The reaction-zone solution is determined by solving the first of Eq. (1) at fixed r; this yields a relationship between the normal front velocity c_n and the local value of r,

$$u(r)=c_n+\epsilon\kappa\,, \tag{4}$$

for interface curvature κ. A graph of the function $u(r)$ is given in Fig. 2(a). In each of the two "smooth" regions, the kinetics are linearized around the value of r corresponding to zero velocity (the "stall" concentration). This reduces the full system to the piecewise linear set

$$\dot{r}_\pm=a_\pm r_\pm+b_\pm \tag{5}$$

with $a_\pm$ and $b_\pm$ calculable from the original kinetics (see Table II). The fast species is directly determined by the slow-species concentration, again with a piecewise linear relationship,

$$\psi^\pm=\psi_0^\pm+d^\pm r^\pm\,. \tag{6}$$

The differential equation (6) is supplemented by the boundary condition (4) at the reaction zone. One can assume uniformly moving reaction zones at $x=0$ ($-$ to $+$) and at $x=\lambda_+,-\lambda_-$ ($+$ to $-$) and derive the traveling-wave dispersion relation relating the widths $\lambda_+,-\lambda_-$ of the quiescent and excited regions to the imposed velocity $\mathbf{c}=c_0\hat{\mathbf{x}}$; this is shown in Fig. 2(b).

The signaling system is only half the story. The system responds to the chemical signal with cell motion and

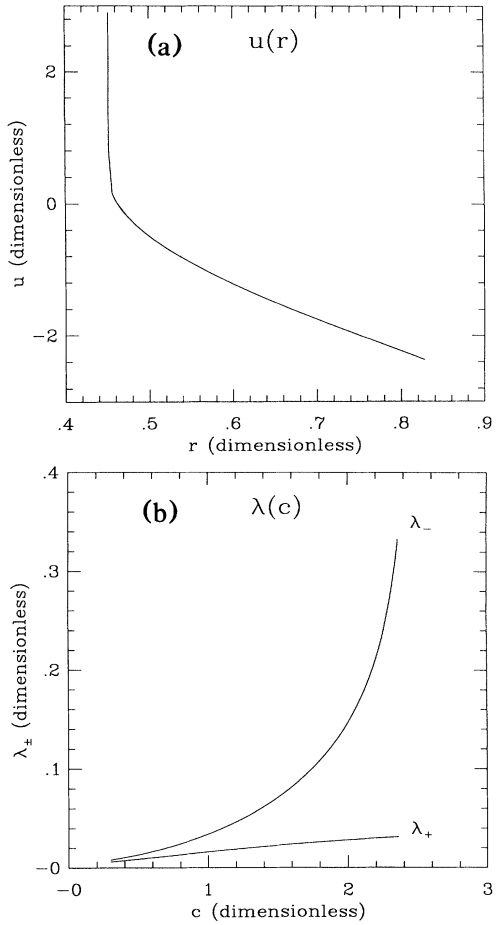

FIG. 2. (a) Plot of the wave velocity u as a function of the receptor concentration in the reaction zone. (b) Plot of the widths of the quiescent, λ_-, and excited, λ_+, phases as a function of the wave speed c.

TABLE I. Parameters for the Martiel-Goldbeter kinetic equations [Eq. (3)].

L_1	10
L_2	0.005
h	18.5
σ	10
λ_1	10^{-3}
λ_2	2.4
s	47
ϵ	0.01
Time scale	28 min
Space scale	8.2 mm

TABLE II. Parameter values ($\pm$) and density dependence ($1\pm$) for the piecewise linear model in the $+$ and $-$ phases.

Parameter	+	−	1_+	1_-
a	−57.80	−10.04	−30.17	−0.749
b	−4.79	3.80	10.20	6.90
d	28.37	9.57×10^{-3}	55.7	4.38×10^{-2}
ψ_0	1.41	2.14×10^{-2}	-3.7×10^{-2}	2.8×10^{-2}
k	0	8.82×10^{-3}	0	0
Γ	14	14	0	0

concomitant density changes. Modeling this coupled system requires an understanding of chemotaxis. This process has been studied in a variety of experiments[12] with the following general conclusions: the cell reacts to cAMP spatial gradients (above a threshold); the response is a function of concentration that is much more sensitive in the low-cAMP state and the cells continue to move for approximately 100 sec after the gradient passes. We generalize the above approach by allowing the cell density ρ to be position dependent and satisfy the continuity equation:

$$\frac{\partial \rho}{\partial t} + \nabla \cdot (\rho \mathbf{v}) = 0 , \tag{7}$$

with cell velocity $\mathbf{v}$.

We close the system by postulating

$$\frac{d\mathbf{v}_\pm}{dt} = -\Gamma \mathbf{v}_\pm + k_\pm \nabla \psi^\pm , \tag{8}$$

where $k_+ \ll k_-$. This equation incorporates the velocity decay and enhanced sensitivity in the quiescent phase. For simplicity, we take $k_+ = 0$ and keep only the large gradient of ψ which occurs as we traverse the reaction zone. The above relationship can then be replaced by the final form

$$\frac{d\mathbf{v}_\pm}{dt} = -\Gamma \mathbf{v}_\pm \tag{9}$$

with the jump condition, across the zone from quiescent to active,

$$[\hat{\mathbf{n}} \cdot \mathbf{v}] = -(k_-/c_n)[\psi] , \tag{10}$$

where $\hat{\mathbf{n}}$ is the normal vector.

Previously, we assumed fixed density. If we substitute that solution into the chemotactic equation, we directly determine the cell velocity $\mathbf{v} = v_0(x)\hat{\mathbf{x}}$. Once v_0 is found, the solution of the continuity equation is

$$\rho_0(z) = \frac{[c - v_0(0)]\rho_0}{c - v_0(x)} . \tag{11}$$

Since the cell velocity is typically a few percent of the wave speed, the density is approximately constant, i.e., the wave dispersion relation is not greatly affected by coupling to cell chemotaxis. However, this is not the case for wave stability.

Let us consider a general two-dimensional perturbation of the planar traveling wave.[13] We introduce the reaction zone shifts:

$$x = \delta_0 e^{iqy} e^{\omega t}, \quad x = \lambda_+ + \delta_1 e^{iqy} e^{\omega t} . \tag{12}$$

There will be similar shifts in the fields $r_\pm$, $\mathbf{v}_\pm$, and $\rho_\pm$. Dropping the common factor $e^{iqy} e^{\omega t}$, we find for the cell velocity

$$\delta \mathbf{v}_\pm(x) = (\hat{\mathbf{x}} \delta v_{x,\pm} - i\hat{\mathbf{y}} \delta v_{y,\pm}) e^{(\omega + \Gamma)x/c} , \tag{13}$$

with constants of integration $\delta v_{x,\pm}$ and $\delta_{y,\pm}$. Substituting this form into the density equation and using the approximation $\rho_0(z) \simeq \rho_0$, we find

$$\frac{\delta \rho_\pm(x)}{\rho_0} = \alpha_\pm e^{\omega x/c} + \left(\frac{q}{c} \delta v_{y,\pm} + \frac{\Gamma + \omega}{c^2} \delta v_{x,\pm} \right) e^{(\Gamma + \omega)x/c} . \tag{14}$$

Again, $\alpha_\pm$ are integration constants.

In the r equation, all of the parameters in the kinetic laws depend on density. The coefficients in the piecewise linear chemical model (5) will all have the generic form $a = a_0 + a_1 \delta\rho$; the linear density dependences are calculated using the parameter definitions given in Ref. 6. Their values are contained in Table II. These terms act as sources for the shifted concentration $\delta r_\pm(x)$. One finds the general solution in terms of two additional unknowns, $\beta_\pm$, and the previously defined coefficients.

The ten unknowns $\alpha_\pm$, $\beta_\pm$, $\delta v_{x,\pm}$, $\delta v_{y,\pm}$, δ_0, and δ_1 are determined by applying the boundary conditions. In detail, we have Eq. (10) and continuity of $\mathbf{v}$ at the jump from active to quiescent phases; Eq. (4) for the chemical concentration at both interfaces; and flux conservation requiring continuity of $\rho(\mathbf{v} \cdot \hat{\mathbf{n}} - c_n)$. Also, the function u which enters in (4) must be expanded to linear order in $\delta\rho$. These conditions determine ten linear equations for the ten (complex) coefficients; the assumed growth rate ω enters explicitly in this system. Setting the determinant to zero gives rise to a highly nonlinear equation for the allowed values of ω.

At $q = 0$, there is a translation mode $\omega = 0$. As q is increased, we can follow this solution branch by using Newton's method with the result at the previous q as the initial guess. We have done this analysis for the parameters given in the tables, at dimensionless velocity equal to 1.746 (corresponding to physical velocity 8.5 μm/sec and oscillation period 5 min); the result is shown in Fig. 3.

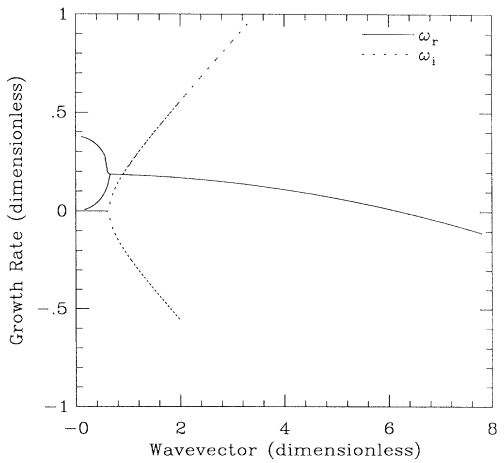

FIG. 3. Plot of the numerically calculated real, ω_r, and imaginary, ω_i, parts of the growth rate of the perturbation as a function of the wave vector of the perturbation, q.

There is a positive growth rate for all q less than some cutoff at around $q=8$. We have checked that there are no other modes with larger $\mathrm{Re}\omega$. By varying several parameters, we have verified that the occurrence of positive growth rates is a generic feature of our system. Thus, the wave pattern is unstable to the formation of transverse structure, possibly with nontrivial time dependence since some unstable modes have $\mathrm{Im}\omega \neq 0$.

What is the physical cause of this instability? It is easy to check that the wave pattern *without* coupling to density fluctuations is stable. Here, though, the effect of a local density increase is enhanced efficacy of the signaling system. This in turn drives chemotaxis towards this site, further increasing the density. As long as the spatial scale of the fluctuation is large enough to prevent the curvature term in (4) from being dominant, the fluctuation will grow.

Let us compare our results to what is seen experimentally.[14] Several hours after initiation of signaling, the concentric target pattern of aggregating cells begins to break up. The cell density loses its axisymmetry and the cells begin to form high-density streams which "flow" towards the central site. In our theory, this is not a transition to instability but instead the growth from an initially small amplitude of an always unstable set of modes. We thus claim that simple aggregation patterns must invariably become more complex. Note though, that the instability's typical growth rate in dimensionless units is 0.25, which in physical units is about 100 min. One would therefore expect to see simple signaling occur over many periods before the instability grows to a perceptible level. Unfortunately, it seems impossible at this point to make a precise quantitative comparison; the experimental results regarding streaming are mostly pictorial. Similarly, we do not as yet know what will happen to our destabilized target pattern for long times.

It would be interesting to investigate this latter issue via numerical simulation.[15] There are, however, several difficulties. The simple linear density dependence that we have assumed here, while adequate for our linear stability analysis, is probably not sufficient for a full nonlinear model. It is also not clear whether the Martiel-Goldbeter model itself is valid over a wide range of density. Another problem arises in the treatment of chemotaxis as the cells begin to aggregate. As the cells start to pile on top of one another, a simple, exponentially decaying velocity is not sufficient, and hydrodynamic effects probably must be taken into consideration.[16] These issues are currently under investigation.

In summary, we have introduced a coupled model of chemical signaling and cell chemotaxis. We can calculate the observed traveling wave pattern and can predict its observed breakup. The streaming instability which we derive is a generic feature of the aggregation dynamics and governs the aggregation pattern on intermediate (several hour) time scales. A full nonlinear theory which would deal with patterns beyond the axisymmetric "target" structure must await further progress in modeling the density dependence of the signaling and chemotaxis systems.

We would like to thank W. Loomis for his useful suggestions and for the photograph of *D. Discoideum.*

[1]James P. Keener and John J. Tyson, Physica (Amsterdam) **21D**, 307–324 (1986).

[2]B. C. Sales, J. E. Turner, and M. B. Maple, Surf. Sci. **114**, 381–394 (1982).

[3]Peter Devreotes, Science **245**, 1054–1058 (1989).

[4]Hanna Parnas and Lee A. Segel, J. Cell Sci. **25**, 191–204 (1977); J. Theor. Biol. **71**, 185–207 (1978); Steven A. Mackay, J. Cell. Sci. **33**, 1–16 (1978).

[5]Evelyn F. Keller and Lee A. Segel, J. Theor. Biol. **26**, 399–415 (1970); P. Grindrod, J. D. Murray, and S. Sinha, IMA J. Math. Appl. Medicine Biol. **6**, 69–79 (1989).

[6]Jean-Louis Martiel and Albert Goldbeter, Biophys. J. **52**, 807–828 (1987).

[7]Michel Darmon and Phillipe Brachet, in *Taxis and Behavior,* edited by G. L. Hazelbauer (Chapman and Hall, London, 1978), pp. 101–139; Peter N. Devreotes and Sally H. Zigmond, Ann. Rev. Cell Biol. **4**, 649–686 (1988).

[8]John J. Tyson and James P. Keener, Physica (Amsterdam) **32D**, 327–361 (1988).

[9]J. J. Tyson, K. A. Alexander, V. S. Manoranjan, and J. D. Murray, Physica (Amsterdam) **34D**, 193–207 (1989).

[10]David A. Kessler and Herbert Levine, Physica (Amsterdam) **39D**, 1–14 (1989).

[11]J. D. Dockery, J. P. Keener, and J. J. Tyson, Physica (Amsterdam) **30D**, 177–191 (1988).

[12]F. Alcantra and M. Monk, J. Gen. Microbiol. **85**, 321–334 (1974); P. R. Fisher, R. Merkl, and G. Gerisch, J. Cell. Biol. **108**, 973–948 (1989); P. J. M. van Haastert, J. Cell. Biol. **96**, 1559–1565 (1983).

[13]D. A. Kessler and H. Levine, Phys. Rev. A **41**, 5418–5430 (1990).

[14]P. C. Newell, in *Biology of the Chemotactic Response,* edited by J. M. Lackie (Cambridge Univ. Press, Cambridge, 1981), pp. 89–114.

[15]See, e.g., D. Barkley, M. Kness, and L. S. Tuckerman, Phys. Rev. A **42**, 2489–2482 (1990); D. Barkley (to be published).

[16]G. M. Odell and J. T. Bonner, Philos. Trans. Roy. Soc. London B **312**, 487–525 (1986).

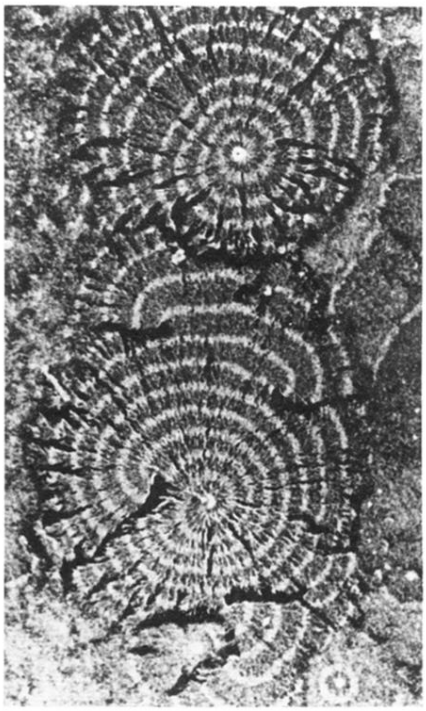

FIG. 1. Photograph of aggregating fields of *D. Discoideum.* Note the spiral signaling patterns and the onset at the aggregations' edges of the streaming instability.